

Multi-spin counter-diabatic driving in many-body quantum Otto refrigerators

Andreas Hartmann,^{1,*} Victor Mukherjee,² Glen Bigan Mbeng,^{1,†} Wolfgang Niedenzu,¹ and Wolfgang Lechner¹

¹*Institut für Theoretische Physik, Universität Innsbruck,
Technikerstraße 21a, A-6020 Innsbruck, Austria*

²*Department of Physical Sciences, IISER Berhampur, Berhampur 760010, India*

(Dated: August 21, 2020)

Quantum refrigerators pump heat from a cold to a hot reservoir. In the few-particle regime, counter-diabatic (CD) driving of, originally adiabatic, work-exchange strokes is a promising candidate to overcome the bottleneck of vanishing cooling power. Here, we present a finite-time many-body quantum refrigerator that yields finite cooling power at high coefficient of performance (CoP), that considerably outperforms its non-adiabatic counterpart. We employ multi-spin CD driving and numerically investigate the scaling behavior of the refrigeration performance with system size. We further prove that optimal refrigeration via the exact CD protocol is a catalytic process.

I. INTRODUCTION

Heat engines and refrigerators are a cornerstone of modern physics and indispensable in today's society [1]. Unravelling their fundamental laws in the few-particle regime has lead to the study of so-called quantum heat engines and refrigerators [2–9]. With the recent progress in controlling quantum systems [10–12], such quantum heat engines could already be experimentally realized using single-body quantum working media [13–18]. Whereas heat engines convert thermal energy into work, their counterparts, namely refrigerators, cool down a cold bath by pumping heat from the cold to the hot reservoir, thereby consuming work [7, 8, 19–24]. The maximum coefficient of performance (CoP) of refrigerators is limited by the Carnot CoP [25]. For these infinitely long (adiabatic) cycle times, the corresponding cooling power naturally converges to zero. A natural question thus arises whether such quantum refrigerators can be driven in finite time, yet produce a finite cooling power.

So called shortcuts to adiabaticity (STA) [26–29] are a promising candidate to overcome this fundamental bottleneck, due to minimizing quantum friction [30–32] during the work-exchange strokes. These STA methods [33–38] including counter-diabatic (CD) driving [38–43] where an additional CD Hamiltonian is applied to suppress any transitions between the system's eigenstates during the Hamiltonian's dynamics, have recently been applied in the field of quantum thermodynamics to enhance the performance of quantum heat engines [44–48] and refrigerators [49, 50] using *single-body* quantum working media (WM). For the latter, *exact* local CD terms can be found analytically [35, 37].

In general, identifying the *exact* counter-diabatic term requires *a priori* knowledge of the system's eigenstates at all times during the Hamiltonian's dynamics and which is numerically and experimentally impractical for *many-body* WM. With this challenge in mind, Sels and Polkovnikov

[41] have developed a variational principle where *approximate* multi-spin CD terms can be found. Based on this method, a quantum heat engine using a *many-body* quantum working medium and local 1-spin CD Hamiltonian could be efficiently implemented [51].

In this work, we present a *finite-time* many-body quantum refrigerator (QR) with *finite cooling power* using additional *approximate multi-spin* counter-diabatic (CD) terms. We numerically demonstrate a large enhancement in cooling power and coefficient of performance (CoP) along with improved scaling behaviour of the cooling power with the system size for the sped-up QR compared to its original non-adiabatic counterpart. For the QR with single-body quantum working medium, we find an analytical expression for the CoP. For the many-body WM, we provide an analytical proof that *exact* CD driving implies a zero work component of the additional external control device. Remarkably, the latter fully assists the piston to run the QR in this case, mimicking the adiabatic quantum cycle, yet in *finite time*.

This work is structured as follows: In Sec. II, we introduce the quantum Otto refrigerator using a many-body spin system as its quantum working medium and present multi-spin local counter-diabatic driving. In Sec. III, we numerically analyze the performance of the corresponding refrigerators and conclude our results in Sec. IV while giving an outlook on future research.

II. METHODS

A. Quantum Otto refrigerator

Quantum Otto refrigerators cyclically pump heat from a cold to a hot reservoir by consuming work. Its corresponding four-stroke quantum Otto cycle [8] consists of two heat-exchange strokes – where the quantum working medium (WM) is alternatingly coupled to two heat baths – and two work-exchange strokes.

The four strokes are (cf. Fig. 1):

1. *Adiabatic compression* ($A \rightarrow B$): Initially, at cold temperature $T_c = 1/\beta_c$, Hamiltonian $H_0(\lambda_c)$ with

* Andreas.Hartmann@uibk.ac.at

† glen.mbeng@uibk.ac.at

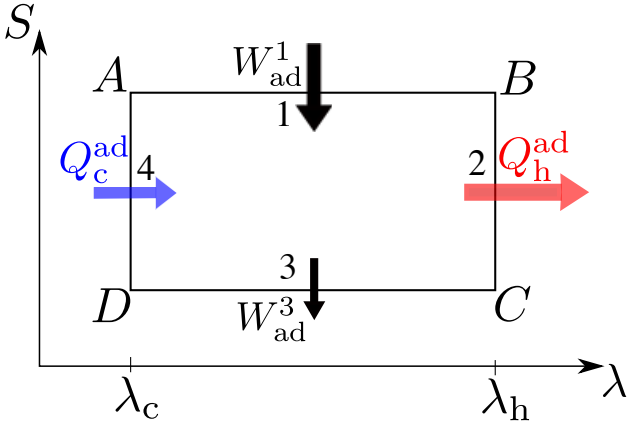


Figure 1. Entropy-working parameter diagram of quantum Otto refrigerator. The quantum Otto cycle consists of two adiabatic (1 and 3) and two thermal strokes (2 and 4). At the end of the cycle, the heat Q_c^{ad} is pumped from the cold bath at temperature T_c into the hot bath at temperature T_h by consuming the work $W_{\text{ad}}^1 + W_{\text{ad}}^3 > 0$.

working parameter $\lambda_c := \lambda(t=0)$ and in the thermal state $\rho_A = e^{-H_0(\lambda_c)/T_c} / \text{Tr}[e^{-H_0(\lambda_c)/T_c}]$, the WM is changed adiabatically during the first isentropic stroke of duration τ_1 with final Hamiltonian $H_0(\lambda_h)$ and mixed state ρ_B with $\lambda_h := \lambda(t=\tau)$.

2. *Hot isochore* ($B \rightarrow C$): The WM is brought in contact with the hot thermal bath at temperature T_h until it equilibrates to the thermal state $\rho_C = e^{-H_0(\lambda_h)/T_h} / \text{Tr}[e^{-H_0(\lambda_h)/T_h}]$. During this heat-exchange stroke of duration τ_2 , the heat Q_h is imparted to the hot bath and the WM's Hamiltonian $H_0(\lambda_h)$ remains unchanged.
3. *Adiabatic expansion* ($C \rightarrow D$): The Hamiltonian $H_0(\lambda_h)$ changes back to $H_0(\lambda_c)$ during the stroke duration τ_3 until the WM attains the state ρ_D .
4. *Cold isochore* ($D \rightarrow A$): The WM is brought in contact with the cold bath at temperature T_c and working parameter λ_c and cools down during the duration τ_4 to its originally initial thermal state ρ_A .

During one cycle, the WM extracts the heat $Q_c^{\text{ad}} := \langle H_0(\lambda_c) \rangle_{\rho_A} - \langle H_0(\lambda_c) \rangle_{\rho_D} > 0$ from the cold thermal bath, thereby consumes the work $W_{\text{ad}}^{1+3} := W_{\text{ad}}^1 + W_{\text{ad}}^3 > 0$ (here, $W_{\text{ad}}^1 = \langle H_0(\lambda_h) \rangle_{\rho_B} - \langle H_0(\lambda_c) \rangle_{\rho_A}$ and $W_{\text{ad}}^3 = \langle H_0(\lambda_c) \rangle_{\rho_D} - \langle H_0(\lambda_h) \rangle_{\rho_C}$). A positive (negative) sign of the work components corresponds to work performed on (extracted from) the WM. Analogously, a positive (negative) sign of the heat corresponds to heat extracted from (imparted to) the thermal bath.

The cooling power is defined as the pumped heat Q_c^{ad} over the total cycle time $\tau_{\text{cycle}} = \sum_{l=1}^4 \tau_l$, i.e.,

$$\mathcal{J}_{\text{ad}} = \frac{\text{pumped heat}}{\text{cycle duration}} = \frac{Q_c^{\text{ad}}}{\tau_{\text{cycle}}}. \quad (1)$$

The coefficient of performance (CoP) of the Otto cycle is defined as the heat Q_c^{ad} pumped from the cold bath over the consumed work $W_{\text{ad}}^1 + W_{\text{ad}}^3$, i.e.,

$$\epsilon_{\text{ad}} = \frac{\text{pumped heat}}{\text{consumed work}} = \frac{Q_c^{\text{ad}}}{W_{\text{ad}}^1 + W_{\text{ad}}^3}. \quad (2)$$

In the adiabatic limit – where the isentropic strokes with durations τ_1 and τ_3 are infinitely long – the cooling power of these *adiabatic* quantum refrigerators goes to zero, i.e., $\lim_{\tau_1, \tau_3 \rightarrow \infty} \mathcal{J}_{\text{ad}} \rightarrow 0$. To overcome this bottleneck, one can implement so called *shortcuts-to-adiabaticity* (STA) techniques for the two work-exchange strokes.

B. Quantum working medium

As our quantum working medium, we consider an all-to-all connected Ising spin chain with Hamiltonian

$$H_0(t) = -[1 - \vartheta(t)] \sum_{j=1}^N h_j \sigma_j^x - \vartheta(t) \left[\sum_{j=1}^N b_j \sigma_j^z + \sum_{j=1}^N \sum_{k < j} J_{jk} \sigma_j^z \sigma_k^z \right] \quad (3)$$

where h_j and b_j , respectively, are the time-dependent transverse and longitudinal magnetic field strengths at site j and J_{jk} the interaction strength between spins at sites j and k . $\vartheta(t)$ is a continuous function that fulfills $\vartheta(t=0) = 0$ and $\vartheta(t=\tau_1) = 1$. For the second isentropic stroke the initial and final values of the function $\vartheta(t)$ are interchanged.

Throughout this work, we parametrize the working parameters λ_c and λ_h with the magnetic fields and interaction strengths at each point of Fig. 1, i.e. $\lambda_c := \{h_{j,i}, b_{j,i}, J_{jk,i}\}$ and $\lambda_h := \{h_{j,f}, b_{j,f}, J_{jk,f}\}$. Here, $h_{j,i}$, $b_{j,i}$ and $J_{jk,i}$ are the values of the magnetic fields and interaction strengths at points A and D , and $h_{j,f}$, $b_{j,f}$ and $J_{jk,f}$ at points B and C , respectively. The explicit forms of the functions $h_j(t)$, $b_j(t)$ and $J_{jk}(t)$ as well as the sweep function $\vartheta(t)$ are given in Appendix A.

C. Multi-spin counter-diabatic driving

The underlying idea of counter-diabatic (CD) driving [38–43] is to efficiently drive an adiabatic evolution of a Hamiltonian in *finite time* by suppressing transitions between its eigenstates. Thus, we always track the instantaneous eigenstates during the whole sweep. Finding the *exact* CD term requires *a priori* knowledge of the system's eigenstates for every time during the sweep which is numerically and experimentally challenging.

In order to overcome this bottleneck, an analytical variational principle has been developed recently [41, 42] to find *approximate* CD terms.

In this work, we drive the WM during the isentropic strokes with the total Hamiltonian

$$H_{\text{STA}}(t) = H_0(t) + H_{\text{CD}}(t) \quad (4)$$

where $H_0(t)$, Eq. (3), is the original non-adiabatic and $H_{\text{CD}}(t)$ the additional counter-diabatic Hamiltonian that suppresses coherences in the WM that cause quantum friction in finite-time sweeps [30–32].

The additional counter-diabatic Hamiltonian reads

$$H_{\text{CD}}(t) = \dot{\vartheta}(t) \mathcal{A}_{\vartheta}(t) \quad (5)$$

with $\mathcal{A}_{\vartheta}(t)$ the *exact* adiabatic gauge potential (AGP) [41, 42, 52] and $\dot{\vartheta}(t)$ the derivative of the sweep function of Eq. (3). We rely on an *approximate* adiabatic gauge potential $\mathcal{A}_{\vartheta}^*$ that contains p -spin terms (with $p \leq N$) and an odd number of σ^y terms (e.g., σ_j^y for $p = 1$, $\sigma_j^y, \sigma_j^y \sigma_k^x$ and $\sigma_j^y \sigma_k^z$ for $p = 2$, etc.). For $p = N$, we obtain the solution of the *exact* adiabatic gauge potential that entails all combinations of N -spin terms (cf. Ref. [53] in the case of quantum criticality). As an example, for $p = 1$ we apply the ansatz $\mathcal{A}_{\vartheta}^* = \sum_{j=1}^N \alpha_j \sigma_j^y$ and solve for the optimal solution of each coefficient α_j by minimizing the operator distance between the exact and approximate AGP. For more details, see Appendix B and Refs. [41, 42, 52].

We note, that we apply the counter-diabatic Hamiltonian *only* in the isentropic strokes as these are normally much longer than the thermalization strokes. However, techniques to speed up the latter have been also developed recently [47, 54–57].

D. Quantum refrigerator under STA

The introduction of the additional *approximate* counter-diabatic term $H_{\text{CD}}^*(t)$ in the Hamiltonian's dynamics during the, originally non-adiabatic, work-exchange strokes requires a careful definition of work, cooling power and coefficient of performance. In Ref. [51], the division

$$W_{\text{STA}}^l := W_0^l + W_{\text{CD}}^l \quad (6)$$

with $W_{\text{STA}}^l \equiv \Delta E = \int_0^{\tau_l} \text{Tr} [\rho(t) \dot{H}_{\text{STA}}(t)] dt$ the total exchanged work for each of the two work-exchange strokes $l \in \{1, 3\}$ with duration τ_l has been introduced. The corresponding work components thus read

$$W_0^l := \int_0^{\tau_l} \text{Tr} [\rho(t) \dot{H}_0(t)] dt, \quad (7)$$

$$W_{\text{CD}}^l := \int_0^{\tau_l} \text{Tr} [\rho(t) \dot{H}_{\text{CD}}(t)] dt \quad (8)$$

where the work W_0^l stems from the piston and W_{CD}^l from the external control device that implements $H_{\text{CD}}^*(t)$.

Remarkably, the work component W_{CD}^l is zero if the additional adiabatic gauge potential and thus the CD Hamiltonian $H_{\text{CD}}^*(t)$ is *exact*, i.e., $\mathcal{A}_{\vartheta}^*(t) = \mathcal{A}_{\vartheta}(t)$ and thus $H_{\text{CD}}^*(t) = H_{\text{CD}}(t)$. In Appendix C, we provide a

detailed proof of this statement. Hence, the work component W_{CD}^{1+3} stemming from the external control device during one cycle can be seen as an artifact of *inexact* CD driving. Experimentally it is advantageous to have a vanishing contribution from the external control device as we want the external control device to fully assist the piston instead of just draining it to run the quantum refrigerator. In other words, the *exact* CD drive is *catalytic* in the sense that it allows for speeding up the cycle without the external control device being altered (charged or discharged) after a cycle.

The cooling power under STA is given by

$$J_{\text{STA}} := \frac{\text{pumped heat}}{\text{cycle duration}} = \frac{Q_c}{\tau_{\text{cycle}}} \quad (9)$$

and the coefficient of performance (CoP) reads

$$\epsilon_{\text{STA}} := \frac{\text{pumped heat}}{\text{consumed work}} = \frac{Q_c}{W_{\text{STA}}^1 + W_{\text{STA}}^3} \quad (10)$$

where $W_{\text{STA}}^{1+3} = W_{\text{STA}}^1 + W_{\text{STA}}^3 > 0$ is the total work performed on (consumed by) the working medium per cycle. Note the difference between the pumped heat Q_c^{ad} for the adiabatic [cf. Eqs. (1) and (2)] and Q_c for the sped-up cycle [cf. Eqs. (9) and (10)].

For the case of a single-body quantum working medium that is modelled by Eq. (3) with $N = 1$, i.e., this reduces to the Landau-Zener (LZ) model, the coefficient of performance evaluates to

$$\epsilon_{\text{LZ}} := \frac{h_{x,i}}{b_{z,f} - h_{x,i}} \quad (11)$$

where $h_{x,i}$ is the initial value of the transverse magnetic field in the first isentropic stroke and $b_{z,f}$ the final value of the longitudinal magnetic field strength, respectively. This expression is positive provided that $b_{z,f} > h_{x,i}$ and is limited by the Carnot CoP $\epsilon_C = T_c/(T_h - T_c)$ [25] (see Appendix D for more details).

III. NUMERICAL RESULTS

In this section, we present the numerical results of the proposed quantum Otto refrigerator. To this end, we used the QuTip 4.2 [58] Python package to simulate the quantum Otto cycle with (i) non-adiabatic [$H_0(t)$, Eq. (3)] and (ii) shortcut-to-adiabaticity (STA) Hamiltonian [$H_{\text{STA}}^*(t)$, Eq. (4)] with p -spin counter-diabatic (CD) terms [$H_{\text{CD}}^*(t)$, Eq. (5)]. We numerically solved the von Neumann equation for the isentropic strokes and computed the heat Q_c and Q_h for the two thermalization strokes as the energy difference between points B and C as well as D and A (cf. Fig. 1), respectively. Throughout this numerical performance analysis, the temperatures for the cold and hot bath are set to $T_c = 0.2$ and $T_h = 0.4$, respectively. The values for the working parameters at points A and D as well as B and C in

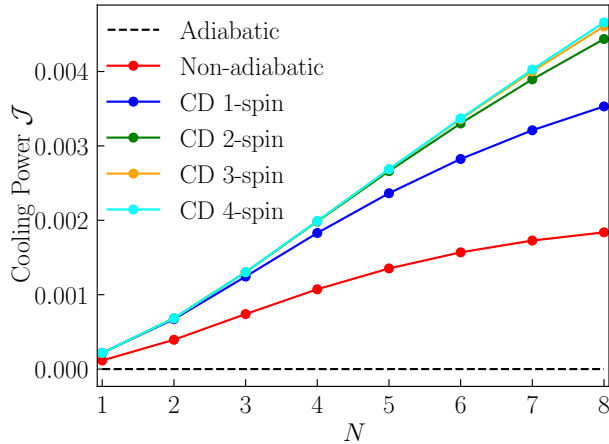


Figure 2. **Cooling power \mathcal{J} over system size N .** Cooling power \mathcal{J} of a quantum Otto cycle for isentropic stroke duration $\tau = \tau_1 = \tau_3 \approx 40$ for (i) non-adiabatic Hamiltonian $[H_0(t)$, Eq. (3)] (red, bottom line) and (ii) shortcut-to-adiabaticity Hamiltonian $[H_{\text{STA}}^*(t)$, Eq. (4)] for different p -spin counter-diabatic terms $[H_{\text{CD}}^*(t)$, Eq. (5)] over different system sizes N . Parameters: Cold and hot bath at temperatures $T_c = 0.2$ and $T_h = 0.4$, respectively, and working parameters λ_c with $h_{j,i} = 0.2$, $b_{j,i} = 0$ and $J_{jk,i} = 0$ and λ_h with $h_{j,f} = 0$, $b_{j,f} = 0.5$ and $J_{jk,f} = 0.1$, magnetic field and interaction strengths, respectively. Duration of the thermalization strokes: $\tau_2 = \tau_4 = 0.1$. Black-dashed line denotes cooling power at adiabatic limit where $\tau = \tau_1 = \tau_3 \rightarrow \infty$.

Fig. 1 read $\lambda_c = \{h_{j,i} = 0.2, b_{j,i} = 0, J_{jk,i} = 0\}$ and $\lambda_h = \{h_{j,f} = 0, b_{j,f} = 0.5, J_{jk,f} = 0.1\}$, respectively, for both, non-adiabatic $H_0(t)$ and shortcut-to-adiabaticity Hamiltonian $H_{\text{STA}}^*(t)$ with p -spin CD Hamiltonian $H_{\text{CD}}^*(t)$ for different p . At each point A, B, C and D , the additionally applied counter-diabatic Hamiltonian is zero, i.e., $H_{\text{CD}}^*(t = \sum_j \tau_j) = 0$ where $j \in \{0, 1, 2, 3\}$ and $\tau_0 = 0$. The durations τ_2 and τ_4 of each thermalization stroke are set to 0.1.

A. Scaling with system size

Our primary goal is to speed up the quantum refrigerator, i.e., we want to pump as much heat Q_c as possible from the cold to the hot reservoir in the shortest amount of time. Thus, we are particularly interested in the cooling power \mathcal{J} during one cycle and its scaling behaviour for different system sizes N .

Figure 2 depicts the cooling power \mathcal{J} for (i) non-adiabatic $[H_0(t)$, Eq. (3)] and (ii) shortcut-to-adiabaticity Hamiltonian $[H_{\text{STA}}^*(t)$, Eq. (4)] for different p -spin counter-diabatic terms $[H_{\text{CD}}^*(t)$, Eq. (5)] over different system sizes N of spins in the working medium for an isentropic stroke duration of $\tau = \tau_1 = \tau_3 \approx 40$. By applying p -spin CD terms, we can efficiently enhance the cooling power of our sped-up refrigerator by increasing the system size N compared to the non-adiabatic counterpart. The relative

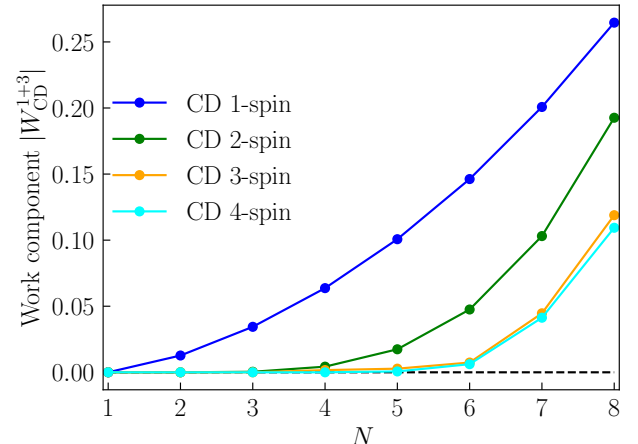


Figure 3. **Work component $|W_{\text{CD}}^{1+3}|$ over system size N for $p \leq 4$.** Absolute value of work component $|W_{\text{CD}}^{1+3}|$ of the shortcut-to-adiabaticity Hamiltonian $[H_{\text{STA}}^*(t)$, Eq. (4)] for different p -spin CD terms $[H_{\text{CD}}^*(t)$, Eq. (5)] over different system sizes N . Parameters: $\tau = \tau_1 = \tau_3 = 1$. Other parameters as in Fig. 2.

enhancement in cooling power decreases the higher p becomes. The major relative enhancement can be made by applying 1-spin or 2-spin CD terms. Including multi-spin terms (e.g. 3 and 4-body in the cases studied) only give a relatively slight improvement compared to 1-spin or 2-spin CD driving. We note, that there is a trade-off between enhanced cooling power with increasing p and implementation complexity for an experiment. In the adiabatic limit (black-dashed line), the cooling power naturally converges to zero.

From a practical point of view, we deem it more favorable if the increased cooling power \mathcal{J}_{STA} is due to the piston rather than draining the external control device. Consequently, we are interested in the work component $|W_{\text{CD}}^{1+3}|$, Eq. (8). As shown in Appendix C the latter is zero if the applied CD Hamiltonian is *exact*.

Figure 3 depicts the absolute value of the work component $|W_{\text{CD}}^{1+3}|$ stemming from the external control device during one cycle for different system sizes N up to $p = 4$. We see that $|W_{\text{CD}}^{1+3}|$ is zero as long as $p > N$. Namely, the CD Hamiltonian must comprise all kinds of interactions up to order N , i.e., involving all the spins in the chain. By contrast, for $N > p$, i.e., more spins N in the WM than order of interaction p in $H_{\text{CD}}^*(t)$, we see that the absolute value of $|W_{\text{CD}}^{1+3}|$ adopts a non-zero value which, according to Appendix C, implies that the Hamiltonian $H_{\text{CD}}^*(t)$ is *not exact* anymore. We therefore conclude, that including a CD Hamiltonian with all combinations up to N -body terms leads to an exact expression when the working medium contains N spins which is consistent with Refs. [41, 42]. These results encourage the goal to strive for an *exact* CD drive. For the latter, the external control device fully assists the piston that optimally “compresses” and “expands” the quantum working medium.

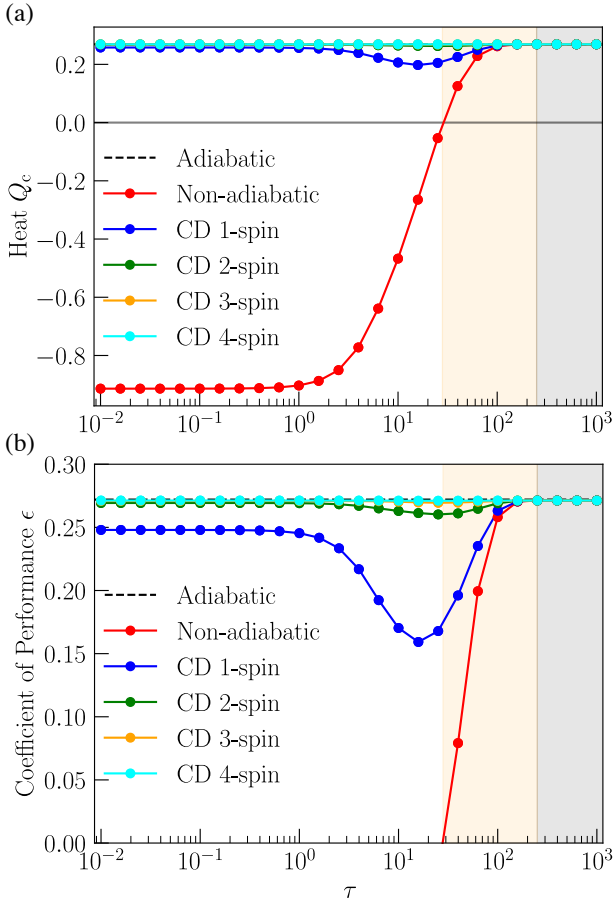


Figure 4. Pumped heat and coefficient of performance. (a) Pumped heat Q_c per cycle and (b) coefficient of performance ϵ for (i) non-adiabatic Hamiltonian [$H_0(t)$, Eq. (3)] and (ii) shortcut-to-adiabaticity Hamiltonian [H_{STA}^* , Eq. (4)] for different p -spin counter-diabatic terms [H_{CD}^* , Eq. (5)] over different isentropic stroke durations $\tau = \tau_1 = \tau_3$ and system size $N = 6$. Yellow-shaded area ($\tau \gtrsim 28$) depicts the refrigerator regime where $Q_c^{na} > 0$ and the gray-shaded area ($\tau \geq 250$) the adiabatic regime where $Q_c^{na} \approx Q_c^{ad}$. Other parameters as in Fig. 2.

B. Dependence on cycle time

We are further interested in the pumped heat Q_c per cycle and the corresponding coefficient of performance (CoP) for different cycle durations τ . Figure 4(a) shows the heat Q_c extracted from the cold reservoir over one cycle for a system size $N = 6$. For the quantum Otto cycle with non-adiabatic Hamiltonian $H_0(t)$, we see that heat $Q_c^{na} > 0$ is pumped from the cold reservoir to the hot bath only for isentropic stroke durations $\tau = \tau_1 = \tau_3 \gtrsim 28$ (yellow-shaded area, refrigerator regime). For shorter isentropic stroke durations, the obtained states ρ'_B and ρ'_D at the end of each isentropic stroke (cf. Fig. 1) are so far away from the ideal adiabatic states ρ_B and ρ_D that the quantum Otto cycle ceases to describe a refrigerator. For large stroke durations, the refrigerator pumps the maximal

possible cooling heat (gray-shaded area, adiabatic regime, $\tau \geq 250$ where $Q_c^{na} \approx Q_c^{ad}$).

By contrast, the sped-up cycle with Hamiltonian $H_{STA}^*(t)$ including 1- up to 4-spin CD terms $H_{CD}^*(t)$ even pumps heat from the cold reservoir in the quench limit $\tau_1, \tau_3 \rightarrow 0$ where the cycle duration is dominated by thermalization. For increasing p , the cooling heat Q_c increases to its maximally possible value Q_c^{ad} for all durations studied. Note, however, that $p = 2$ appears to be efficient even for the intermediate regime where $p = 1$ does not yield optimal results. This is in accordance with Fig. 2. Note that for the adiabatic regime, the strength of the additional $H_{CD}^*(t)$ converges to zero (as $\dot{\vartheta}(t) \propto 1/\tau$, cf. Appendix A) and hence $Q_c \rightarrow Q_c^{ad}$.

Figure 4(b) depicts the corresponding coefficient of performance (CoP) ϵ , Eq. (10). For the sped-up cycle with $H_{STA}^*(t)$, Eq. (4), we see that the higher p -spin terms we use for our CD Hamiltonian $H_{CD}^*(t)$, Eq. (5), the larger the CoP becomes. Note that the CoP appears to be more sensitive to the value of p than the pumped heat Q_c . Namely, converging to the optimal CoP ϵ^{ad} , Eq. (2), generally requires a larger p than for the optimal extracted heat Q_c^{ad} which is due to a non-zero W_{CD}^{1+3} .

IV. DISCUSSION AND OUTLOOK

In this work, we have presented a *many-body* quantum Otto refrigerator that efficiently operates at *finite-time*. The many-body quantum working medium (WM) is modelled by an all-to-all connected Ising spin chain where the working parameter is parametrized via magnetic fields and interactions. In order to speed up the quantum Otto cycle, we apply an additional *approximate* counter-diabatic (CD) Hamiltonian. The latter outperforms its non-adiabatic counterpart in pumped heat per cycle. The additional CD Hamiltonian contains p -spin terms with an odd number of σ^y terms and $p \leq N$. For $p = N$, we obtain the *exact* CD Hamiltonian. We provide an analytical proof and give numerical evidence that the work component stemming from the external control device is *zero* if the CD Hamiltonian is *exact*. In this case, the external control device fully assists the piston to pump heat from a cold to a hot reservoir. Note that while an *exact* CD protocol implies zero work contribution from the external control device over a cycle, the converse, however, is not true. It is therefore not possible to find an exact CD Hamiltonian via minimizing this work component.

We numerically demonstrate an enhanced cooling power and coefficient of performance (CoP) for the sped-up quantum Otto refrigerator with higher p -spin CD driving compared to its non-adiabatic counterpart. Furthermore, we show that increasing p improves the scaling behaviour in cooling power with system size. For the Otto cycle with single-body quantum WM, i.e., described via the Landau-Zener model, we find an analytical expression for the CoP that only depends on the applied magnetic field strengths. The analytical and numerical performance

analysis reveals that quantum Otto refrigerators can be scaled up efficiently by increasing the number of spins in the working medium.

The results presented in this work disclose some important operational features. We note that there is a trade-off between experimental feasibility of the additionally applied CD terms and vanishing work component stemming from the external control device. For the latter, we need to apply non-local multi-spin CD terms (for example through additional laser fields) that are hard to implement in current experiments. On the other hand, applying only local 1-body CD terms may result in enhanced cooling power compared to its non-adiabatic counterpart, yet under the price of extensive use of the external control device rather than the piston.

We note that several cost identifiers for the additional CD Hamiltonian have been introduced [45, 46, 48, 50, 59–62]. We note, further, that these *implementational* costs are conceptually different to the *operational* costs described by the work W_{CD}^{1+3} stemming from the external control device [51]. In fact, in the case of *exact* CD driving we go on the optimal, i.e., adiabatic, path from points *A* to *B* and *C* to *D* in Fig. 1, respectively. Although the operational cost will then be zero, i.e., $W_{\text{CD}}^{1+3} = 0$, there will still be a cost of *implementing* the additional CD Hamiltonian.

For future research, we intend to study the robustness of the applied CD protocols with respect to external noise and possible cooperative effects [63]. Further, we aim at developing a *many-body* quantum refrigerator where work and heat exchanges occur simultaneously.

ACKNOWLEDGEMENTS

We thank Adolfo del Campo for valuable discussions. W. N. acknowledges support from an ESQ fellowship of the Austrian Academy of Sciences (ÖAW). V. M. acknowledges support from Science and Engineering Research Board (SERB) through Start-up Research Grant (Project No.SRG/2019/000411) and from Seed grant of IISER Berhampur. Work was supported by the Austrian Science Fund (FWF) through a START grant under Project No. Y1067-N27 and the SFB BeyondC Project No. F7108-N38, the Hauser-Raspe foundation, and the European Union’s Horizon 2020 research and innovation program under grant agreement No. 817482. This material is based upon work supported by the Defense Advanced Research Projects Agency (DARPA) under Contract No. HR001120C0068. Any opinions, findings and conclusions or recommendations expressed in this material are those of the author(s) and do not necessarily reflect the views of DARPA.

Appendix A: Protocols for magnetic fields and interactions

For the many-body quantum working medium in the text, the explicit time dependence of the magnetic field and interaction strengths for the non-adiabatic $[H_0(t)$, Eq. (3)] and shortcut-to-adiabaticity Hamiltonian $[H_{\text{STA}}^*(t)$, Eq. (4)] read

$$h_j(t) = h_{j,i} + (h_{j,f} - h_{j,i})\vartheta(t), \quad (\text{A1a})$$

$$b_j(t) = b_{j,i} + (b_{j,f} - b_{j,i})\vartheta(t), \quad (\text{A1b})$$

$$J_{jk}(t) = J_{jk,i} + (J_{jk,f} - J_{jk,i})\vartheta(t) \quad (\text{A1c})$$

where

$$\vartheta(t) := \sin^2 \left[\frac{\pi}{2} \sin^2 \left(\frac{\pi t}{2\tau_l} \right) \right] \quad (\text{A2})$$

is the sweep function and $h_{j,i} = h_j(t=0)$, $b_{j,i} = b_j(t=0)$, $J_{jk,i} = J_{jk}(t=0)$ and $h_{j,f} = h_j(t=\tau_l)$, $b_{j,f} = b_j(t=\tau_l)$, $J_{jk,f} = J_{jk}(t=\tau_l)$ the initial and final values for each isentropic stroke $l \in \{1, 3\}$ of duration τ_l , respectively. Its derivative with respect to time reads

$$\dot{\vartheta}(t) = \frac{\pi^2}{4\tau_l} \sin \left(\frac{\pi}{\tau_l} t \right) \sin \left[\pi \sin^2 \left(\frac{\pi}{2\tau_l} t \right) \right] \quad (\text{A3})$$

and is applied to the CD Hamiltonian, Eq. (5).

Appendix B: Multi-spin CD driving

For the counter-diabatic Hamiltonian $H_{\text{CD}}(t)$, Eq. (5) in the text, we apply an *approximate* adiabatic gauge potential \mathcal{A}_ϑ^* . Here, we follow the variational method introduced in Ref. [41].

We make an ansatz \mathcal{A}_ϑ^* with p -spin Pauli matrices and an odd number of σ^y terms for the adiabatic gauge potential (AGP) and calculate the Hermitian operator $G_\vartheta(\mathcal{A}_\vartheta^*) = \partial_\vartheta H_0 + i[\mathcal{A}_\vartheta^*, H_0]$. The goal is to minimize the operator distance $D^2(\mathcal{A}_\vartheta^*) = \text{Tr}\{[G_\vartheta(\mathcal{A}_\vartheta) - G_\vartheta(\mathcal{A}_\vartheta^*)]^2\}$ between the exact, \mathcal{A}_ϑ , and approximate AGP, \mathcal{A}_ϑ^* . This minimization is equivalent to minimizing the action

$$S(\mathcal{A}_\vartheta^*) = \text{Tr}[G_\vartheta^2(\mathcal{A}_\vartheta^*)] \quad (\text{B1})$$

with respect to its parameters in front of every Pauli matrix term, i.e., $\delta S(\mathcal{A}_\vartheta^*)/\delta \mathcal{A}_\vartheta^* = 0$.

As an example, for $p = 1$, i.e., 1-spin CD driving, we apply the ansatz $\mathcal{A}_\vartheta^* = \sum_{j=1}^N \alpha_j \sigma_j^y$ and calculate the Hermitian operator $G_\vartheta(\mathcal{A}_\vartheta^*)$ as well as the action $S(\mathcal{A}_\vartheta^*)$. By minimizing the latter with respect to the coefficients α_j , we find the optimal solution for each spin. For $p = 2$, we apply the ansatz $\mathcal{A}_\vartheta^* = \sum_{j=1}^N \alpha_j \sigma_j^y + \sum_{k < j} \beta_{jk} (\sigma_j^y \sigma_k^z + \sigma_j^z \sigma_k^y) + \gamma_{jk} (\sigma_j^y \sigma_k^x + \sigma_j^x \sigma_k^y)$ and solve the corresponding action with respect to all coefficients α_j , β_{jk} and γ_{jk} . With this variational method, we can also include multi-spin terms, potentially up to N -body terms $\sigma_1^z \cdots \sigma_j^y \cdots \sigma_N^x$. We solve the optimal form of each coefficient numerically.

Appendix C: Proof of zero work component W_{CD} for exact CD driving

Here, we provide a detailed proof to the statement that the work contribution [51]

$$W_{\text{CD}}^l := \int_0^{\tau_l} \text{Tr} [\rho(t) \dot{H}_{\text{CD}}(t)] dt \quad (\text{C1})$$

stemming from the external control device for each isentropic stroke $l \in \{1, 3\}$ becomes *zero* if the additionally applied counter-diabatic Hamiltonian $H_{\text{CD}}^*(t)$ is *exact*. The latter reads [34]

$$H_{\text{CD}}(t) = i\hbar \sum_n |\partial_t n\rangle\langle n| - \langle n|\partial_t n\rangle|n\rangle\langle n| \quad (\text{C2})$$

where $|n\rangle$ denotes the instantaneous eigenstate at time t . The density matrix $\rho(t)$ can be written as

$$\rho(t) = \sum_n a_n(t) |n\rangle\langle n| \quad (\text{C3})$$

where $a_n(t)$ is a time-dependent coefficient. Here, we have used that under exact CD driving the density matrix remains diagonal in the instantaneous eigenbasis [64].

We now calculate the integral over the energy function

$$f(t) := \text{Tr}[\rho(t) \dot{H}_{\text{CD}}(t)] \quad (\text{C4})$$

for one isentropic stroke of duration τ (where $\dot{H}_{\text{CD}}(t=0) = \dot{H}_{\text{CD}}(t=\tau) = 0$). By applying the following relations (using $\sum_n |n\rangle\langle n| = \mathbb{1}$)

$$\sum_n \partial_t^2 (|n\rangle\langle n|) = |\partial_t^2 n\rangle\langle n| + 2|\partial_t n\rangle\langle \partial_t n| + |n\rangle\langle \partial_t^2 n| = 0, \quad (\text{C5a})$$

$$|\partial_t n\rangle\langle \partial_t n| = -\frac{1}{2} (|n\rangle\langle \partial_t^2 n| + |\partial_t^2 n\rangle\langle n|), \quad (\text{C5b})$$

$$\begin{aligned} \partial_t(\langle n|n\rangle) &= \langle \partial_t n|n\rangle + \langle n|\partial_t n\rangle = 0, \\ \langle \partial_t n|n\rangle &= -\langle n|\partial_t n\rangle, \\ 2\langle n|\partial_t n\rangle &= \langle n|\partial_t n\rangle + \langle n|\partial_t n\rangle = \langle n|\partial_t n\rangle - \langle \partial_t n|n\rangle, \end{aligned} \quad (\text{C5c})$$

the time-derivative of the Hamiltonian $H_{\text{CD}}(t)$ reads

$$\begin{aligned} \partial_t H_{\text{CD}}(t) &= i\hbar \sum_n |\partial_t^2 n\rangle\langle n| + |\partial_t n\rangle\langle \partial_t n| - \partial_t(\langle n|\partial_t n\rangle|n\rangle\langle n|) \\ &\stackrel{(\text{C5a})}{=} i\hbar \sum_n \frac{1}{2} (|\partial_t^2 n\rangle\langle n| - |n\rangle\langle \partial_t^2 n|) - \partial_t(\langle n|\partial_t n\rangle)|n\rangle\langle n| \\ &\quad - \langle n|\partial_t n\rangle(|\partial_t n\rangle\langle n| + |n\rangle\langle \partial_t n|). \end{aligned} \quad (\text{C6})$$

The function $f(t) = \text{Tr}[\rho(t) \dot{H}_{\text{CD}}(t)]$, Eq. (C4), can consequently be rewritten (using $\text{Tr}[\hat{H}] = \sum_n \langle n|\hat{H}|n\rangle$) as

$$\begin{aligned} f(t) &= i\hbar \sum_n a_n \left[\frac{1}{2} (\langle n|\partial_t^2 n\rangle - \langle \partial_t^2 n|n\rangle) - \partial_t(\langle n|\partial_t n\rangle) - \langle n|\partial_t n\rangle (\langle n|\partial_t n\rangle + \langle \partial_t n|n\rangle) \right] \\ &\stackrel{(\text{C5b})}{=} \frac{i\hbar}{2} \sum_n a_n [\langle n|\partial_t^2 n\rangle - \langle \partial_t^2 n|n\rangle - 2\partial_t(\langle n|n\rangle)] \\ &\stackrel{(\text{C5c})}{=} \frac{i\hbar}{2} \sum_n a_n [\langle n|\partial_t^2 n\rangle - \langle \partial_t^2 n|n\rangle - \partial_t(\langle n|\partial_t n\rangle - \langle \partial_t n|n\rangle)] \\ &= \frac{i\hbar}{2} \sum_n a_n [\langle n|\partial_t^2 n\rangle - \langle \partial_t^2 n|n\rangle - \langle \partial_t n|\partial_t n\rangle - \langle n|\partial_t^2 n\rangle + \langle \partial_t^2 n|n\rangle + \langle \partial_t n|\partial_t n\rangle] \\ &= 0 \end{aligned} \quad (\text{C7})$$

which proves the statement above.

Fig. 1) of the cycle. It reads

Appendix D: Single-body working medium

In analogy to Ref. [48], we derive the coefficient of performance (CoP) of the quantum refrigerator with a single-body working medium.

The CoP, Eq. (10), in the text can be rewritten in terms of the energies E_i with $i \in \{A, B, C, D\}$ at each point (cf.

$$\epsilon_{\text{LZ}} = \frac{E_A - E_D}{E_B - E_A + E_D - E_C} = \frac{1}{\frac{E_B - E_C}{E_A - E_D} - 1} \quad (\text{D1})$$

where the energies are

$$\begin{aligned} E_A &= -h_{x,i} \tanh\left(\frac{h_{x,i}}{T_c}\right), \\ E_B &= -b_{z,f} \tanh\left(\frac{h_{x,i}}{T_c}\right), \\ E_C &= -b_{z,f} \tanh\left(\frac{b_{z,f}}{T_h}\right), \\ E_D &= -h_{x,i} \tanh\left(\frac{b_{z,f}}{T_h}\right), \end{aligned} \quad (\text{D2})$$

due to the uniform scaling of the energy levels in this two-level system after each stroke. Inserting the latter, Eq. (D1) consequently reads

$$\epsilon_{\text{LZ}} = \frac{1}{\frac{b_{z,f}}{h_{x,i}} - 1} \quad (\text{D3})$$

which is equivalent to Eq. (11) from the text.

The pumped heat

$$Q_c = E_A - E_D = h_{x,i} \left[\tanh\left(\frac{b_{z,f}}{T_h}\right) - \tanh\left(\frac{h_{x,i}}{T_c}\right) \right] \geq 0 \quad (\text{D4})$$

is positive for the Otto cycle to describe a refrigerator. From the latter and the fact that \tanh is a monotonously increasing function, it follows that

$$\frac{b_{z,f}}{h_{x,i}} \geq \frac{T_h}{T_c}. \quad (\text{D5})$$

Inserting this into Eq. (D3), we finally obtain

$$\epsilon_{\text{LZ}} = \frac{1}{\frac{b_{z,f}}{h_{x,i}} - 1} \leq \frac{1}{\frac{T_h}{T_c} - 1} = \frac{T_c}{T_h - T_c} = \epsilon_c. \quad (\text{D6})$$

[1] Y. A. Çengel and M. A. Boles, *Thermodynamics: An Engineering Approach*, eighth ed. (McGraw-Hill Education, New York, 2015).

[2] R. Alicki, The quantum open system as a model of the heat engine, *J. Phys. A* **12**, L103 (1979).

[3] R. Kosloff, A quantum mechanical open system as a model of a heat engine, *J. Chem. Phys.* **80**, 1625 (1984).

[4] R. Kosloff, Quantum Thermodynamics: A Dynamical Viewpoint, *Entropy* **15**, 2100 (2013).

[5] D. Gelbwaser-Klimovsky, W. Niedenzu, and G. Kurizki, Thermodynamics of Quantum Systems Under Dynamical Control, *Adv. At. Mol. Opt. Phys.* **64**, 329 (2015).

[6] S. Vinjanampathy and J. Anders, Quantum thermodynamics, *Contemp. Phys.* **57**, 1 (2016).

[7] B. Karimi and J. P. Pekola, Otto refrigerator based on a superconducting qubit: Classical and quantum performance, *Phys. Rev. B* **94**, 184503 (2016).

[8] R. Kosloff and Y. Rezek, The Quantum Harmonic Otto Cycle, *Entropy* **19** (2017), 10.3390/e19040136.

[9] F. Binder, L. A. Correa, C. Gogolin, J. Anders, and G. Adesso, eds., *Thermodynamics in the Quantum Regime* (Springer, Cham, 2019).

[10] H. Bernien, S. Schwartz, A. Keesling, H. Levine, A. Omran, H. Pichler, S. Choi, A. S. Zibrov, M. Endres, M. Greiner, V. Vuletić, and M. D. Lukin, Probing many-body dynamics on a 51-atom quantum simulator, *Nature* **551**, 579 (2017).

[11] J.-y. Choi, S. Hild, J. Zeiher, P. Schauß, A. Rubio-Abadal, T. Yefsah, V. Khemani, D. A. Huse, I. Bloch, and C. Gross, Exploring the many-body localization transition in two dimensions, *Science* **352**, 1547 (2016).

[12] P. Bordia, H. Lüschen, S. Scherg, S. Gopalakrishnan, M. Knap, U. Schneider, and I. Bloch, Probing Slow Relaxation and Many-Body Localization in Two-Dimensional Quasiperiodic Systems, *Phys. Rev. X* **7**, 041047 (2017).

[13] J. V. Koski, V. F. Maisi, J. P. Pekola, and D. V. Averin, Experimental realization of a Szilard engine with a single electron, *Proc. Natl. Acad. Sci. USA* **111**, 13786 (2014).

[14] J. Roßnagel, S. T. Dawkins, K. N. Tolazzi, O. Abah, E. Lutz, F. Schmidt-Kaler, and K. Singer, A single-atom heat engine, *Science* **352**, 325 (2016).

[15] J. Klaers, S. Faelt, A. Imamoglu, and E. Togan, Squeezed Thermal Reservoirs as a Resource for a Nanomechanical Engine beyond the Carnot Limit, *Phys. Rev. X* **7**, 031044 (2017).

[16] J. P. S. Peterson, T. B. Batalhão, M. Herrera, A. M. Souza, R. S. Sarthour, I. S. Oliveira, and R. M. Serra, Experimental Characterization of a Spin Quantum Heat Engine, *Phys. Rev. Lett.* **123**, 240601 (2019).

[17] D. von Lindenfels, O. Gräß, C. T. Schmiegelow, V. Kaushal, J. Schulz, M. T. Mitchison, J. Goold, F. Schmidt-Kaler, and U. G. Poschinger, Spin Heat Engine Coupled to a Harmonic-Oscillator Flywheel, *Phys. Rev. Lett.* **123**, 080602 (2019).

[18] J. Klatzow, J. N. Becker, P. M. Ledingham, C. Weinzel, K. T. Kaczmarek, D. J. Saunders, J. Nunn, I. A. Walmsley, R. Uzdin, and E. Poem, Experimental Demonstration of Quantum Effects in the Operation of Microscopic Heat Engines, *Phys. Rev. Lett.* **122**, 110601 (2019).

[19] Y. Rezek, P. Salamon, K. H. Hoffmann, and R. Kosloff, The quantum refrigerator: The quest for absolute zero, *EPL (Europhysics Letters)* **85**, 30008 (2009).

[20] A. Levy and R. Kosloff, Quantum Absorption Refrigerator, *Phys. Rev. Lett.* **108**, 070604 (2012).

[21] Y. Yuan, R. Wang, J. He, Y. Ma, and J. Wang, Coefficient of performance under maximum χ criterion in a two-level atomic system as a refrigerator, *Phys. Rev. E* **90**, 052151 (2014).

[22] R. Long and W. Liu, Performance of quantum Otto refrigerators with squeezing, *Phys. Rev. E* **91**, 062137 (2015).

[23] O. Abah and E. Lutz, Optimal performance of a quantum Otto refrigerator, *EPL (Europhysics Letters)* **113**, 60002 (2016).

[24] W. Niedenzu, I. Mazets, G. Kurizki, and F. Jendrzejewski, Quantized refrigerator for an atomic cloud, *Quantum* **3**, 155 (2019).

[25] H. B. Callen, *Thermodynamics and an introduction to thermostatics* (Wiley, New York, 1985).

[26] E. Arimondo, P. R. Berman, and C. C. Lin, eds., *Advances in Atomic, Molecular, and Optical Physics*, Adv. At. Mol. Opt. Phys., Vol. 62 (Academic Press, 2013) pp. 117 – 169.

[27] A. del Campo and K. Sengupta, Controlling quantum critical dynamics of isolated systems, *The European Physical Journal Special Topics* **224**, 189 (2015).

[28] A. del Campo and K. Kim, Focus on Shortcuts to Adiabaticity, *New Journal of Physics* **21**, 050201 (2019).

[29] D. Guéry-Odelin, A. Ruschhaupt, A. Kiely, E. Torrontegui, S. Martínez-Garaot, and J. G. Muga, Shortcuts to adiabaticity: Concepts, methods, and applications, *Rev. Mod. Phys.* **91**, 045001 (2019).

[30] R. Kosloff and T. Feldmann, Discrete four-stroke quantum heat engine exploring the origin of friction, *Phys. Rev. E* **65**, 055102 (2002).

[31] T. Feldmann and R. Kosloff, Quantum four-stroke heat engine: Thermodynamic observables in a model with intrinsic friction, *Phys. Rev. E* **68**, 016101 (2003).

[32] T. Feldmann and R. Kosloff, Quantum lubrication: Suppression of friction in a first-principles four-stroke heat engine, *Phys. Rev. E* **73**, 025107 (2006).

[33] M. Demirplak and S. A. Rice, Adiabatic Population Transfer with Control Fields, *The Journal of Physical Chemistry A*, *The Journal of Physical Chemistry A* **107**, 9937 (2003).

[34] K. Takahashi, Transitionless quantum driving for spin systems, *Phys. Rev. E* **87**, 062117 (2013).

[35] X. Chen, A. Ruschhaupt, S. Schmidt, A. del Campo, D. Guéry-Odelin, and J. G. Muga, Fast Optimal Frictionless Atom Cooling in Harmonic Traps: Shortcut to Adiabaticity, *Phys. Rev. Lett.* **104**, 063002 (2010).

[36] X. Chen, E. Torrontegui, and J. G. Muga, Lewis-Riesenfeld invariants and transitionless quantum driving, *Phys. Rev. A* **83**, 062116 (2011).

[37] K. Takahashi, Transitionless quantum driving for spin systems, *Phys. Rev. E* **87**, 062117 (2013).

[38] C. Jarzynski, Generating shortcuts to adiabaticity in quantum and classical dynamics, *Phys. Rev. A* **88**, 040101 (2013).

[39] A. del Campo, Shortcuts to Adiabaticity by Counterdiabatic Driving, *Phys. Rev. Lett.* **111**, 100502 (2013).

[40] B. Damski, Counterdiabatic driving of the quantum Ising model, *Journal of Statistical Mechanics: Theory and Experiment* **2014**, P12019 (2014).

[41] D. Sels and A. Polkovnikov, Minimizing irreversible losses in quantum systems by local counterdiabatic driving, *Proc. Natl. Acad. Sci. USA* **114**, E3909 (2017).

[42] P. W. Claeys, M. Pandey, D. Sels, and A. Polkovnikov, Floquet-Engineering Counterdiabatic Protocols in Quantum Many-Body Systems, *Phys. Rev. Lett.* **123**, 090602 (2019).

[43] A. Hartmann and W. Lechner, Rapid counter-diabatic sweeps in lattice gauge adiabatic quantum computing, *New J. Phys.* **21**, 043025 (2019).

[44] A. d. Campo, J. Goold, and M. Paternostro, More bang for your buck: Super-adiabatic quantum engines, *Scientific Reports* **4**, 6208 EP (2014).

[45] O. Abah and E. Lutz, Performance of shortcut-to-adiabaticity quantum engines, *Phys. Rev. E* **98**, 032121 (2018).

[46] O. Abah and M. Paternostro, Shortcut-to-adiabaticity Otto engine: A twist to finite-time thermodynamics, *Phys. Rev. E* **99**, 022110 (2019).

[47] L. Dupays, I. L. Egusquiza, A. del Campo, and A. Chenu, Superadiabatic thermalization of a quantum oscillator by engineered dephasing, *Phys. Rev. Research* **2**, 033178 (2020).

[48] B. Çakmak and Ö. E. Müstecapoglu, Spin quantum heat engines with shortcuts to adiabaticity, *Phys. Rev. E* **99**, 032108 (2019).

[49] K. Funo, N. Lambert, B. Karimi, J. P. Pekola, Y. Matsuoka, and F. Nori, Speeding up a quantum refrigerator via counterdiabatic driving, *Phys. Rev. B* **100**, 035407 (2019).

[50] O. Abah, M. Paternostro, and E. Lutz, Shortcut-to-adiabaticity quantum Otto refrigerator, *Phys. Rev. Research* **2**, 023120 (2020).

[51] A. Hartmann, V. Mukherjee, W. Niedenzu, and W. Lechner, Many-body quantum heat engines with shortcuts to adiabaticity, *Phys. Rev. Research* **2**, 023145 (2020).

[52] M. Kolodrubetz, D. Sels, P. Mehta, and A. Polkovnikov, Geometry and non-adiabatic response in quantum and classical systems, *Phys. Rep.* **697**, 1 (2017).

[53] A. del Campo, M. M. Rams, and W. H. Zurek, Assisted Finite-Rate Adiabatic Passage Across a Quantum Critical Point: Exact Solution for the Quantum Ising Model, *Phys. Rev. Lett.* **109**, 115703 (2012).

[54] S. Alipour, A. Chenu, A. T. Rezakhani, and A. del Campo, Shortcuts to Adiabaticity in Driven Open Quantum Systems: Balanced Gain and Loss and Non-Markovian Evolution, (2019), arXiv:1907.07460 [quant-ph].

[55] R. Dann, A. Tobalina, and R. Kosloff, Fast route to equilibration, *Phys. Rev. A* **101**, 052102 (2020).

[56] R. Dann, A. Tobalina, and R. Kosloff, Shortcut to Equilibration of an Open Quantum System, *Phys. Rev. Lett.* **122**, 250402 (2019).

[57] A. Das and V. Mukherjee, Quantum-enhanced finite-time Otto cycle, *Phys. Rev. Research* **2**, 033083 (2020).

[58] J. R. Johansson, P. D. Nation, and F. Nori, QuTiP 2: A Python framework for the dynamics of open quantum systems, *Comput. Phys. Commun.* **184**, 1234 (2013).

[59] O. Abah and E. Lutz, Energy efficient quantum machines, *EPL (Europhysics Letters)* **118**, 40005 (2017).

[60] S. Campbell and S. Deffner, Trade-Off Between Speed and Cost in Shortcuts to Adiabaticity, *Phys. Rev. Lett.* **118**, 100601 (2017).

[61] Y. Zheng, S. Campbell, G. De Chiara, and D. Poletti, Cost of counterdiabatic driving and work output, *Phys. Rev. A* **94**, 042132 (2016).

[62] A. Tobalina, I. Lizuain, and J. G. Muga, Vanishing efficiency of a speeded-up ion-in-Paul-trap Otto engine, *EPL (Europhysics Letters)* **127**, 20005 (2019).

[63] A. Manatuly, W. Niedenzu, R. Román-Ancheyta, B. Çakmak, Ö. E. Müstecapoglu, and G. Kurizki, Collectively enhanced thermalization via multiqubit collisions, *Phys. Rev. E* **99**, 042145 (2019).

[64] K. Funo, J.-N. Zhang, C. Chatou, K. Kim, M. Ueda, and A. del Campo, Universal Work Fluctuations During Shortcuts to Adiabaticity by Counterdiabatic Driving, *Phys. Rev. Lett.* **118**, 100602 (2017).